Agricultural and Forest Meteorology 151 (2011) 1453–1461

Contents lists available at ScienceDirect

Agricultural and Forest Meteorology

journal homepage: www.elsevier.com/locate/agrformet

Documenting improvement in leaf area index estimates from MODIS using hemispherical photos for Australian savannas

William B. Sea[a,*], Philippe Choler[b], Jason Beringer[c], Richard A. Weinmann[d], Lindsay B. Hutley[d], Ray Leuning[a]

[a] CSIRO Marine and Atmospheric Research, Canberra, ACT, Australia
[b] Université Joseph Fourier, Grenoble, France
[c] Monash University, Melbourne, Victoria, Australia
[d] Charles Darwin University, Darwin, Northern Territory, Australia

ARTICLE INFO

Article history:
Received 2 August 2010
Received in revised form 5 November 2010
Accepted 14 December 2010

Keywords:
LAI
Savannas
MODIS validation
Hemispherical photos

ABSTRACT

This paper compares estimates of Leaf Area Index (LAI) obtained from the MODIS (Moderate Resolution Imaging Spectroradiometer) collections 4.8 (MC4) and 5.0 (MC5) with ground-based measurements taken along a 900 km north–south transect through savanna in the Northern Territory, Australia. There was excellent agreement for both the magnitude and timing in the annual variation in LAI from MC5 and biometric estimates at Howard Springs, near Darwin, whereas MC4 overestimated LAI by 1–2 m^2 m^{-2} for the first 200 days of the year. Estimates of LAI from MC5 were also compared with those obtained from the analysis of digital hemispherical photographs taken during the dry season (September 2008) based on algorithms that included random and clumped distribution of leaves. Linear regression of LAI from MC5 versus that using the clumping algorithm yielded a slope close to 1 ($m = 0.98$). The regression based on a random distribution of leaves yielded a slope significantly different from 1 ($m = 1.37$), with higher Mean Absolute Error (MAE) and bias compared to the clumped analysis. The intercept for either analysis was not significantly different from zero but inclusion of five additional sites that were visually bare or without green vegetation produced a statistically significant offset of +0.16 m^2 m^{-2} by MC5. Overall, our results show considerable improvement of MC5 over MC4 LAI and good agreement between MC5 and ground-based LAI estimates from hemispherical photos incorporating clumping of leaves.

1. Introduction

Leaf Area Index (LAI), defined as half the total leaf area per unit ground area (Chen and Black, 1992), is an essential input for many studies concerned with the exchanges of radiation, heat, mass and momentum between the land and atmosphere (Asner et al., 2003; Yang et al., 2006a; Demarty et al., 2007). Accurate knowledge of LAI is required for land surface schemes in climate models (Cramer et al., 1999; Sitch et al., 2008; Stockli et al., 2008), for simple models of evapotranspiration (Cleugh et al., 2007; Leuning et al., 2008), and for improving models of global phenology (e.g. Kang et al., 2003; Arora and Boer, 2005). Most of these applications require weekly to monthly variation of LAI at spatial scales ranging from tens of meters to hundreds of kilometers. Because of their global coverage and continuous monitoring, remotely sensed radiances measured by satellites have increasingly been used to estimate LAI at these temporal and spatial scales (Gower et al., 1999; Myneni et al., 2002; Garrigues et al., 2008). A number of remotely sensed LAI data products exist at global coverage: CYCLOPES (Baret et al., 2007), GLOBCARBON (Global Land Products for Carbon Model Assimilation, Bacour et al., 2006), AVHRR (Advanced Very High Resolution Radiometer, Ganguly et al., 2008) and MODIS (Moderate resolution Imaging Spectrometer, Myneni et al., 2002).

However, the utility of satellite-based LAI measurements can only be fully recognized if they are properly validated. Recent validation studies have used high spatial resolution remote sensing imagery (e.g. IKONOS, Landsat, or Satellite Pour l'Observation de la Terre (SPOT)) to generate reference maps of LAI via a transfer function between a vegetation index such as NDVI (Normalized Difference Vegetation Index) and LAI (Morisette et al., 2006). These reference maps are then aggregated for comparison with moderate-scale LAI products from AVHRR or MODIS (Cohen et al., 2006; Morisette et al., 2006; Yang et al., 2006b). While the use of high spatial resolution imagery to validate LAI at larger scales shows great promise, ground-based measurements are required to develop scaling relationships between LAI and NDVI. With appropriate statistical design, this paper demonstrates that ground-based measurements of LAI can also be

* Corresponding author. Tel.: +61 02 6246 5619.
E-mail address: w_sea@yahoo.com (W.B. Sea).

0168-1923/$ – see front matter © 2011 Elsevier B.V. All rights reserved.
doi:10.1016/j.agrformet.2010.12.006

used directly to validate the remotely sensed LAI products from MODIS.

Early methods to estimate LAI included destructive harvesting and leaf litter traps (see Breda, 2003 review), point quadrats (Warren Wilson, 1963), and the Adelaide technique (Andrew et al., 1979). Indirect optical techniques are also commonly used, such as hemispherical photographs (e.g. Jonckheere et al., 2004; Leblanc et al., 2005; Macfarlane et al., 2007a,b), the TRAC (Wave Energy, INC), the LAI-2000 canopy analyzer (LI-COR Inc., Lincoln, Nebraska) or the DEMON (Lang and Xiang, 1986). Yang et al. (2006b) suggested that validation of MODIS solely with ground-based measurements is unsatisfactory because of expense in terms of time and sampling effort, while further complications include mismatch of spatial scales by the two approaches, vegetation heterogeneity and geolocation errors (Jonckheere et al., 2004; Tan et al., 2006; Yang et al., 2006a).

These are not fundamental objections because they can be addressed by well-designed spatial sampling strategies and modern geolocation technologies. Selection of relatively homogeneous forests and woodlands avoids problems of vegetation heterogeneity when using ground-based techniques to validate MODIS LAI products (Cohen et al., 2003; Kang et al., 2003; Wang et al., 2004; Fang and Liang, 2005; Morisette et al., 2006; Zhang et al., 2003). For these ecosystems, the older MODIS collection 4.8 LAI product correctly captures the seasonal LAI dynamics but produces unrealistically high LAI maxima (Leuning et al., 2005; Kanniah et al., 2009). Validating remotely sensed LAI products for tropical savannas (Privette et al., 2002; Scholes et al., 2004; Huemmrich et al., 2005; Hill et al., 2006; Kanniah et al., 2009) is difficult given the significant spatial heterogeneity of these tree-grass ecosystems. The problem of ground-based validation of MODIS LAI in savannas can be overcome by sampling across long transects within a given pixel to account for landscape heterogeneity. In the case of using hemispherical digital photographs many images are required to obtain an accurate estimate of LAI, a somewhat tedious process that has been simplified by the recent development of freely available software (Baret and Weiss, 2004; Fuentes et al., 2009). A further advantage of digital images is that the data can be retained for further reprocessing if new analysis techniques become available (Weiss et al., 2004).

In this study we use remotely sensed LAI data from both the older MODIS collection 4.8 (MC4) and the current collection 5.0 (MC5). From the initial version of the MODIS LAI algorithm (Knyazikhin et al., 1999), improvements have occurred in the form of collections. The first three collections derived LAI using a land cover map based on AVHRR data (Cohen et al., 2006), with later collections based on MODIS land cover (Yang et al., 2006b). Earlier work investigating the performance of MODIS LAI found problems with overestimating LAI for herbaceous canopies and excessive reliance on a backup algorithm (due to image contamination by clouds) for woody vegetation during the growing season (Shabanov et al., 2005). Later algorithms for LAI retrievals (collection 4.8) corrected for overestimation of LAI in herbaceous canopies. The current collection 5 (MC5) distinguishes between deciduous and evergreen broadleaf forests and optimizes retrievals for all biomes using a new, stochastic radiative transfer algorithm to correct for previous problems with woody vegetation LAI including correcting for vegetation clumping (Shabanov et al., 2007). There are as yet few published reports to confirm this expected improvement (Kanniah et al., 2009). This study compares the two MODIS LAI products against digital hemispherical photos and earlier ground-based LAI data (O'Grady, 2000). We then examine the performance of the newest MODIS LAI collection using hemispherical photographs taken at 24 savanna sites along a 900 km north–south transect from northern Australia. The sampling here was undertaken in conjunction with an intensive field campaign held in September 2008 (late dry season) called the "Savanna Patterns of Energy and Carbon Integrated Across the Landscape" (SPECIAL) campaign.

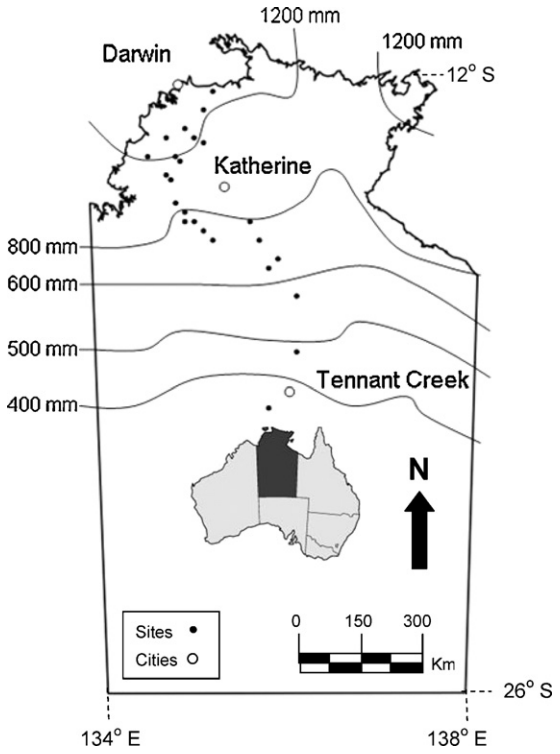

Fig. 1. The location of field sites estimating LAI using digital hemispherical photos in the Northern, Territory, Australia. Isohyets (mm yr^{-1}) are shown for median annual rainfall (1961–90). Climate data courtesy of the Australian Bureau of Meteorology.

2. Materials and methods

2.1. Site description

The vast expanse of grasslands, savannas, and woodlands in northern Australia provides an ideal landscape to validate MODIS LAI products. This is due to the strong rainfall gradient (decreasing inland) which produces changes in LAI and because Australian savannas are arguably the most intact in the world (Woinarski et al., 2007). Previous research established the Northern Australian Tropical Transect (NATT) to examine a number of ecological relationships between rainfall and soil texture and vegetation structure including tree cover, stem basal area, and tree height (Williams et al., 1996; Cook et al., 2002). Changes in floristic composition and structure are provided by Williams et al. (1996). Annual average rainfall along the transect decreases from 1700 mm/yr at Darwin to 450 mm/yr approximately 900 km southeast at Tennant Creek (Fig. 1). The region experiences a distinct dry season lasting from five to eight months and a wet season for the remainder of the year. The overall climatology is provided by Cook and Heerdegen (2001). Tree cover (and LAI) tends to be higher in wetter regions closer to the sea in the north and reduces towards the interior of the continent (Cook et al., 2002; Hill et al., 2006). Evergreen eucalyptus trees (e.g. *Eucalyptus tetrodonta* and *Eucalyptus miniata*) dominate the overstory throughout much of the region, with deciduous understory shrubs and small tree species more numerous in the north (Williams et al., 1997). Annual variation in LAI is composed of a somewhat steady contribution from evergreen tree species, a large amplitude from annual and perennial grasses in response to higher soil moisture during the rainy season, and a small seasonal cycle from deciduous and semi-deciduous trees that increase leaf area in

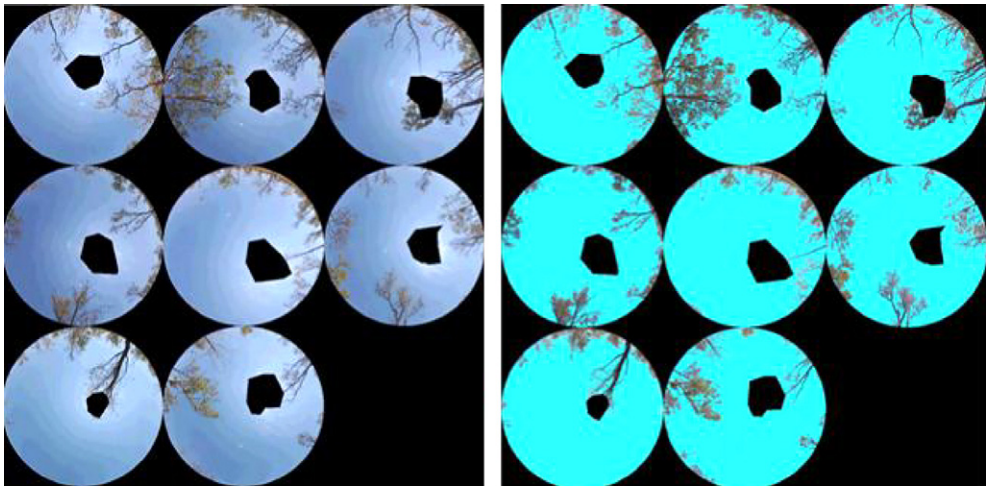

Fig. 2. Examples of digital hemispherical photos analyzed using the CAN_EYE 5.0 software. Images on the left are originals and those on the right have been edited into separate classes for vegetation and sky. The black mask excludes contamination by the sun or camera operator.

advance of the seasonal rains (Williams et al., 1997; O'Grady et al., 2000; Lu et al., 2003; Hill et al., 2006). It should be noted that our study was undertaken during the dry season when the grasses had completely senesced and therefore the LAI reported here generally represents the LAI of trees only.

2.2. Ground based LAI

2.2.1. Digital hemispherical photographs and on-ground sampling strategy

Digital Hemispherical Photographs (DHPs) for LAI measurements were taken within 24 (1-km) pixels located along a 900 km transect in the Northern Territory, Australia, running from a savanna woodland at Howard Springs, just east of Darwin, to a largely grassland site near Tennant Creek (Fig. 1). The measurements were made from 2 to 15 September 2008 as part of a large-scale field campaign designed to measure fluxes of heat, water vapor and CO_2 at landscape scale. The MODIS pixels were chosen to be representative of the vegetation at each of seven core sites that had flux towers, whereas the others were selected for accessibility while excluding those with topographic anomalies such as rivers, highways, and human disturbances that may lead to unacceptable sampling errors.

Approximately 80 digital images were taken within each georeferenced MODIS pixel along a triangular sampling transect positioned using a GPS instrument (Garmin Trex©). The first 400 m transect was directed from the edge of the pixel towards its centre, from which a second 400 m transect radiated out at a random angle (45–135°, 225–315°). Finally, a longer third transect returned to the starting point. Hemispherical photographs were taken approximately every 20 m along the transect using a Nikon D40 camera equipped with a 4.5 mm Sigma circular fisheye lens and focal length set to infinity. The camera was pointed upwards at a height approximately 25 cm above ground or just above the senescent grass.

2.2.2. DHP data processing

A recent software package, CAN_EYE version 5.0 (Baret and Weiss, 2004), was used to estimate both *effective* LAI and *true* LAI from unidirectional gap fractions based on hemispherical photos. The effective LAI is computed assuming a Poisson random gap and leaf angle distribution, whereas the true LAI is computed using a leaf clumping algorithm based on Lang and Xiang (1986) (see Demarez et al., 2008 for details). To avoid any confusion in nomenclature between the algorithms, we will call the two approaches, non-clumped LAI and clumped LAI, respectively. Several studies have recommended obtaining gap fraction measurements at a 57.5° viewing angle from zenith (Jonckheere et al., 2004; Demarez et al., 2008). This gap fraction is relatively independent of leaf angle distribution and allows direct estimation of the non-clumped LAI (Jonckheere et al., 2004). Estimates of LAI at this viewing angle are thus likely to be more robust than when sampling with other angles which are complicated by various combinations of sun and leaf angles during the day. Some studies suggest that clumping-based LAI is the appropriate one for comparison with MC5 LAI (Shabanov et al., 2007; Huang et al., 2008).

The CAN_EYE software includes an automatic image classification scheme allowing, in theory, for quite rapid processing of a series of photos. Images were analyzed in batches of 15–20. First, a mask (appearing black in Fig. 2) excludes contamination of the digital image by the sun or camera operator. Next, a sky pixel is selected by the operator and the software automatically classifies similar sky pixels based on color shading. The supervised classification process ends when new sky pixels are indistinguishable from plant material. Using gap-fraction analysis of the photos, and assuming a random spatial distribution of leaves and a 57.5° viewing angle with respect to nadir, non-clumped LAI were computed for each photograph. Fig. 2 provides an example of eight digital photos where the supervised classification has enhanced the contrast between vegetation and sky to aid subsequent analysis of the image.

2.2.3. Partitioning leaf from stem area

The LAI derived from DHPs should strictly be called Plant Area Index (PAI) because light from the sky is absorbed by leaves, stems and branches. The stochastic radiative transfer algorithm for the MODIS MC5 LAI product calculates *green* leaf area index and thus comparison of remotely sensed LAI with ground-based measurements requires PAI to be partitioned into leaf and woody fractions. The fraction of green LAI to PAI was estimated using CAN_EYE to reprocess a subset of DHPs representative of the entire transect. We stress that the following comparisons are green LAI from MC5 with leaf area from the hemispherical photos.

2.3. Remote sensing data

2.3.1. MODIS

MODIS LAI (MOD15A2) data were obtained from the Oak Ridge National Laboratory Distributed Active Archive Center MODIS website (http://daac.ornl.gov/MODIS/modis.html). The MODIS algorithm calculates LAI by using the highest daily value of fPAR (fraction of absorbed Photosynthetically Active Radiation) in each 8-day composite period. fPAR values are converted into LAI using a six-biome classification map and vegetation structural parameters in a lookup table. The nominal spatial resolution for the MODIS LAI product is 1 km. For comparison between MC4 and MC5, only LAI data of the highest quality were used, thus rejecting any data with cloud contamination or those obtained using the backup algorithm. MC5 estimates of LAI were compared to estimates using hemispherical photos sampled within each MODIS pixel (see Table 1 for descriptions). To assess the appropriateness of our ground-based sampling techniques to capture the spatial variability within a MODIS pixel, we first examined viewing angles of the MODIS satellite for field locations in our study. Greater viewing angles imply successively larger ground area represented by each MODIS pixel. The viewing angles were <10° from vertical, and the small viewing angle, plus the finding that adjacent MC5 LAI values had very similar values shows that our ground sampling was representative of individual MODIS pixels.

2.3.2. Aggregating up using Landsat data to reference maps

Morisette et al. (2006) proposed a standard protocol for validating moderate-scale remotely sensed LAI values at 1-km resolution using ground-based measurements (e.g. DHPs) combined with higher resolution (<30 m) remote sensing data from Landsat or SPOT. This allows construction of aggregated LAI reference maps to account for the spatial heterogeneity within each 1-km pixel. To assess the spatial heterogeneity in LAI within our 24 pixels we used freely available Landsat Enhanced Thematic Mapper 7+ (ETM7+) radiances (http://glovis.usgs.gov) for the dates without cloud contamination closest to our DHP measurements (for corresponding Landsat dates, see Table 1). The red and near-infrared bands in the Landsat ETM7+ tiles were subsampled to the 1-km MODIS scale using MultiSpec (http://cobweb.ecn.purdue.edu/~biehl/MultiSpec). These two bands were used to calculate NDVI, and the variance in NDVI was rescaled to match the observed range in LAI from analysis of the DHPs. The spatial variation in LAI within each pixel is thus proportional to the re-scaled NDVI. We examined the spatial variability within a MODIS pixel by assessing how the Coefficient of Variation (CV) in Landsat-derived NDVI changes as aggregated plot area increases. We found that CV in NDVI decreases until aggregated plot length reaches 200 m, and then remains stable. Finally, we compared the CV in Landsat NDVI with DHP LAI for each MODIS pixel, and found similar results for each sampling approach, showing that our ground-based DHP sampling strategy adequately captures the spatial variability found within a MODIS pixel.

2.3.3. Statistical methods

Variability in our ground-based LAI measurements was examined in three ways. Firstly, we assume: (i) that the 80 DHPs adequately sample the spatial heterogeneity within each MODIS pixel and (ii) that the LAI values are normally distributed. Thus the 95% confidence limits are given by the mean ± 2 standard errors. The second approach computes the 95% confidence intervals using a Monte Carlo bootstrapping method to sample, with replacement, the DHP LAI values 1000 times for each MODIS pixel. In the third approach, confidence intervals were estimated from the spatial variability in the aggregated reference maps from Landsat ETM7+. Uncertainties in the MC5 LAI data were estimated by temporally averaging two 8-day periods before and after the date closest to our ground-based measurements.

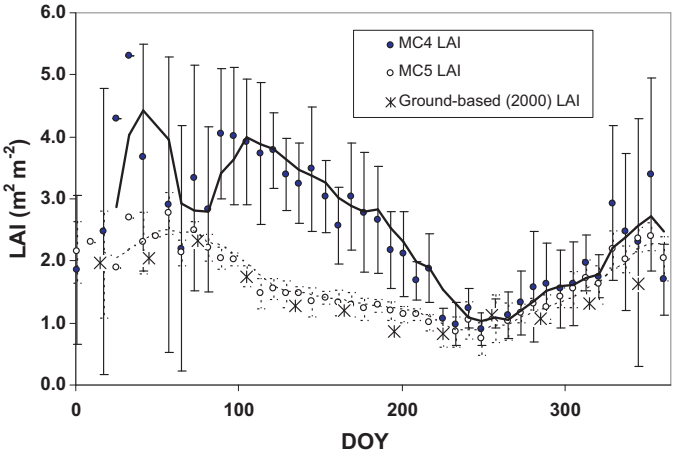

Fig. 3. Average seasonal variation of LAI at Howard Springs, Northern Territory for 2000–2006 as given by MC4 and MC5 data products. Ground-based measurements for 2000 derived from combined overstory (O'Grady, 2000) and understory (Hutley and Williams, unpublished data) LAI are also shown. Lines represent 24 day moving averages of mean values for the period 2000–2006 for only the highest quality LAI retrievals from MODIS, i.e. no cloud contamination or reliance on the back-up algorithm. Vertical lines represent ±1 standard deviations around the mean.

Standard Major Axis (SMA) regression analysis was used to compare LAI estimated using DHPs and from MODIS. SMA regression analysis accounts for uncertainties in both sets of measurements and allows testing the statistical significance of any deviation of the slope from unity and the intercept from zero (Warton et al., 2006). Of particular interest are comparisons of MODIS LAI with values obtained using the random non-clumped or clumped leaf area distribution algorithms in the CAN_EYE software.

3. Results

3.1. LAI time series of MOD15A2 collections 4 and 5 and ground-based measurements

Fig. 3 compares the seasonal variability in MC4 and MC5 with LAI measurements at the Howard Springs eddy flux tower site reported by O'Grady et al. (2000). They used the Adelaide technique (Andrew et al., 1979) that counts the number of tree branches and estimates LAI through knowledge of the average leaf mass per branch and the specific leaf area. There is an excellent correlation between the seasonal variation in LAI estimates from MC5 and those from the surface observations. In contrast, MC4 significantly overestimates LAI from Day Of Year (DOY) 1 to 230, with two peaks around 4.0 on DOY 40 and DOY 110 compared to a peak of ~2.4 at DOY 65 from MC5 and the ground-based observations. Furthermore, MC4 shows a rapid increase in LAI commencing around day 90 with a very slow decline thereafter, whereas the other two data sets show a smaller increase in LAI and lower rate of decline. Standard errors in both MC4 and MC5 are very large in the wet season (DOY 270 – 075) possibly due to large amounts of cloud contamination in the data. Consequently, LAI from the two collections differ significantly only between days 90 and 210. Our results are in agreement with a recently published study that was based on monthly LAI and only two years of MC5 data (Kanniah et al., 2009) at Howard Springs.

3.2. Converting PAI from hemispherical photos into LAI

Fig. 4 shows stem wood fraction (area of wood to PAI) as a function of tree cover fraction (one minus the fraction of pixels

Table 1
Latitude, longitude, vegetation class, sampling date, Leaf Area Index (LAI) from MC5 and DHPs from sites sampled in the Northern Territory. For the SPECIAL campaign, Site 1 corresponds to Dry River, Sturt Plains Woodland (12), Howard Springs (15), Adelaide River (16), Daly River Uncleared (21). Dates for corresponding Landsat imagery were 13 September (Sites 1–8, 21–24), 30 August (9–13), 29 September (14–20).

Site	Latitude	Longitude	Vegetation	Sampling date (2008)	MC5 LAI	DHP LAI
1	−15.2542	132.3693	Eucalyptus	12 September	0.8	0.9
2	−15.2625	132.3660	Eucalyptus	12 September	0.9	1.0
3	−15.2875	132.2608	Eucalyptus	12 September	0.7	0.7
4	−15.1625	132.1046	Eucalyptus	12 September	1.1	1.1
5	−15.0542	132.0717	Eucalyptus	12 September	0.8	0.9
6	−14.9458	131.9617	Eucalyptus	12 September	0.8	0.5
7	−15.0974	133.0312	Eucalyptus	13 September	0.9	0.8
8	−15.6173	133.2465	Eucalyptus	13 September	0.6	0.6
9	−19.0008	134.1741	Acacia	14 September	0.2	0.1
10	−19.7212	134.1336	Acacia	14 September	0.3	0.2
11	−17.8279	133.8478	Acacia	15 September	0.2	0.3
12	−17.1301	133.3181	Acacia	15 September	0.4	0.3
13	−17.0715	133.4518	Acacia	15 September	0.5	1.0
14	−12.5208	131.2009	Evergreen Forest	2 September	2.3	2.1
15	−12.8205	131.1465	Eucalyptus	4 September	1.0	1.0
16	−13.0792	131.1209	Eucalyptus	5 September	0.7	0.6
17	−13.0708	131.1209	Eucalyptus	5 September	0.7	0.4
18	−13.0292	131.0975	Eucalyptus	5 September	1.1	1.0
19	−13.0292	130.9264	Eucalyptus	6 September	0.9	0.7
20	−13.1531	130.7708	Eucalyptus	6 September	1.2	0.7
21	−14.0208	131.3953	Eucalyptus	10 September	1.0	1.0
22	−14.0208	131.4039	Eucalyptus	10 September	1.1	0.9
23	−13.8625	131.3138	Eucalyptus	10 September	1.0	0.6
24	−13.8708	131.3013	Eucalyptus	10 September	0.8	0.8

in each DHP classified sky) computed by CAN_EYE. The slope of the linear regression is 0.214 ($r^2 = 0.957$, $p < 0.01$), from which we infer that $LAI_{non\text{-}clumped} = 0.786 * PAI$, on the assumption that the wood material and leaves are distributed randomly throughout the canopy. This relationship is used to convert PAI to green LAI in what follows.

3.3. Collection 5 versus hemispherical photos

Fig. 5a shows that there is a strong linear relationship between LAI derived from hemispherical photos and those from MC5. The SMA slope of the linear regression of LAI from MC5 versus LAI from CAN_EYE is 1.37 when clumping is ignored but is 0.98 when the clumping algorithm is used. The SMA regression relationship also indicates a positive offset for MC5 LAI for the non-clumped (0.089) and clumped cases (0.035), but the offsets are not statistically significant at $p = 0.05$ (Table 2). Although the relationships have approximately the same r^2 for the non-clumped (0.887) and clumped (0.881) CAN_EYE algorithms, Table 2 shows that the Mean Absolute Error (MAE) and Mean Square Error (MSE) are both sub-

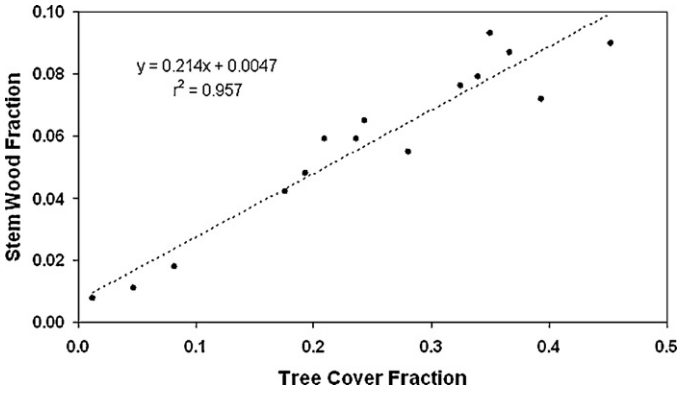

Fig. 4. Relationship between total tree cover and the stem wood cover. The slope of the linear regression is 0.214 ($r^2 = 0.957$, $p < 0.01$). By inference, if woody material and leaf material are distributed approximately evenly through the canopy, $LAI_{non\text{-}clumped} = 0.79 * PAI$.

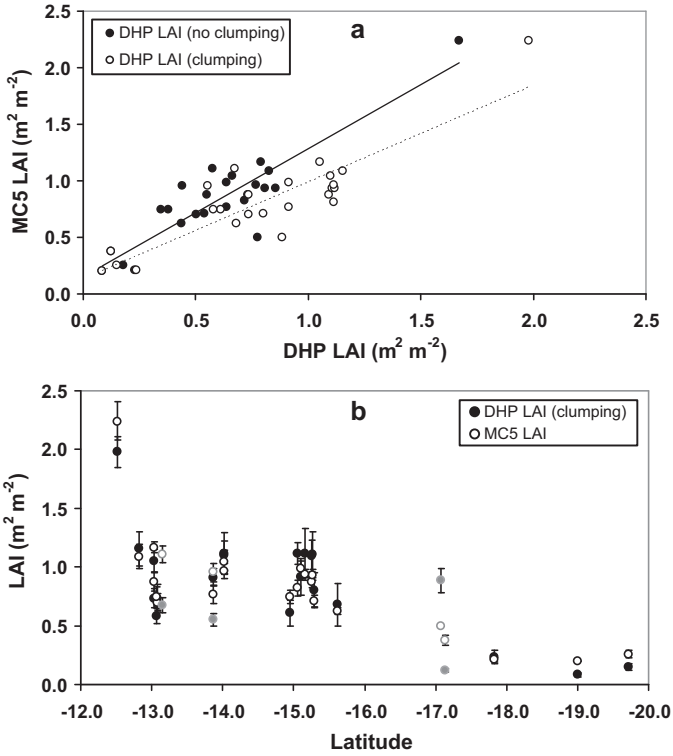

Fig. 5. (a) Standard Major Axis (SMA) regression between LAI obtained from MC5 LAI and using the random and clumping algorithms of CAN_EYE to analyze DHPs. The linear regression of LAI from MC5 (y) versus that using the clumping algorithm to analyze the hemispherical photos (x) yielded $y = 0.98x + 0.035$, $r^2 = 0.881$, $p < 0.01$, and $y = 1.37x + 0.0089$, $r^2 = 0.887$, $p < 0.01$ (random algorithm). (b) Latitudinal variation of LAI for the 24 sites along the NATT from the DHPs and MC5. Bars on the DHP LAI indicate 95% confidence intervals constructed using reference maps of NDVI from Landsat ETM7+ Normalized Difference Vegetation Index (NDVI) data. Bars on the MC5 LAI indicate 95% confidence intervals constructed by using values from ±2 periods around the ground sampling period. Outliers are highlighted in gray.

Table 2
Summary statistics for Standardized Major Axis (SMA) regression analysis ($y = mx + b$) comparing LAI from hemispherical photos (x) and MC5 (y). Shown are correlation coefficients (r^2) and confidence intervals on the slopes and intercepts of SMA regression using CAN_EYE algorithms without and with clumping for vegetated sites only and including non-vegetated sites (including zeros). For the SMA intercept b, $p > 0.05$ indicates a non-significant offset. For the slope m, $p < 0.05$ indicates a slope statistically indistinguishable from 1. The Mean Square Error (MSE) is partitioned into systematic MSE_s (bias) and unsystematic MSE_u (random) components. Mean Absolute Error (MAE) is also shown.

Case	n	r^2	SMA intercept b	H_0: $b = 0$ p value	SMA slope m	H_0: $m = 1$ p value
Intercept different from 0, slope different from 1						
Non-clumped	24	0.887	0.089	0.312	1.367	0.005
Clumped	24	0.881	0.035	0.709	0.986	0.896
Including zeros	29	0.899	0.146	0.028	0.884	0.161

Case	MSE ($m^4\ m^{-4}$)	MSE_s ($m^4\ m^{-4}$)	MSE_u ($m^4\ m^{-4}$)	MAE ($m^2\ m^{-2}$)
Model performance (errors $m^2\ m^{-2}$)				
Non-clumped	0.122	0.086	0.036	0.306
Clumped	0.042	0.004	0.038	0.168
Including zeros	0.051	0.015	0.036	0.188

Case	Low m	High m	Low b	High b
95% confidence intervals on slopes (m) and intercepts (b)				
Non-clumped	1.109	1.683	−0.089	0.267
Clumped	0.797	1.221	−0.158	0.228
Including zeros	0.741	1.054	0.017	0.275

stantially lower for LAI estimated using CAN_EYE with clumping compared to non-clumping. The MSE for the clumped algorithm is largely unsystematic (random), while the non-clumped MSE is dominated by systematic error (bias).

To examine further if MODIS LAI has an offset problem, we located five sites devoid of any standing green vegetation and of sufficient size to cover the MODIS pixel footprint. We found a modest non-zero offset, with LAI values ranging from 0.2 to 0.5 $m^2\ m^{-2}$, and a mean of 0.28 $m^2\ m^{-2}$ (Table 3). When these additional sites are included in the SMA regression (clumped case), the offset is significantly different from zero, with a SMA intercept of 0.146 ($p = 0.03$).

LAI from MC5 was then compared in Fig. 5b to the estimates of LAI obtained along the latitudinal gradient by analyzing hemispherical photos with CAN_EYE software for clumped cases. Standard errors of LAI estimated from DHPs were within ±0.5 $m^2\ m^{-2}$ for all sites, and except for two sites, LAI from MC5 was within ±2 standard errors of the mean LAI from the DHPs (not shown). All but four MC5 values were within the computed 95% confidence intervals of the mean LAI obtained from transects of hemispherical photos and within-pixel spatial variances calculated using Landsat ETM7+ data (Fig. 5b). Similar standard error estimates were obtained using Monte Carlo bootstrapping derived from our hemispherical photos, confirming that our sampling methods using Monte Carlo methods to compute confidence intervals provided a complementary approach to using reference NDVI maps.

3.4. Patterns of LAI in the Northern Territory

Fig. 6 shows LAI from MC5 along a continuous transect from 12.5° S to 19.5° S for periods typical of the wet (DOY 89) and dry (DOY 279) seasons (Fig. 6). There is a great contrast between LAI in the wet and dry seasons along the entire transect, with wet season LAI approximately twice the value for the dry season. The dates chosen correspond to the earliest date (Day 89) that MC5 LAI data is reliably free of cloud contamination and Day 257, which is approximately the same date as the field campaign for this study. The geographic patterns are striking in that LAI is not linearly related to Mean Annual Precipitation (MAP), but instead LAI declines rapidly inland from the coast inland for 100 km and then has a pronounced plateau over much of the transect even though mean annual precipitation decreases from 1200 to 600 mm. South of the plateau, there is another rapid drop in LAI to very low levels where annual precipitation is less than 400 mm.

4. Discussion

Given the large spatial areas of tropical woodlands, savannas, and grasslands worldwide, reducing uncertainty in estimates of LAI will help improve global modeling of carbon and water exchange (Chapin et al., 2002). Our study highlights another improvement in LAI retrievals since the beginning of the MODIS LAI algorithms (Knyazikhin et al., 1999). Our results are in agreement with an earlier study documenting problems of overestimation in LAI for MC4 in Australian savannas and woodlands (Hill et al., 2006). We found considerable improvement for both the magnitude and timing for MC5 compared to MC4 at Howard Springs (Fig. 3). The results from Figs. 3 and 6 show the dynamic nature of LAI in savannas, where the contribution from the understory (grasses and deciduous shrubs) in the wet season often exceeds that from the overstory. At all but four of our sites MODIS LAI values were within the 95% confidence intervals for mean LAI estimates by hemispherical photos (Fig. 5b). These four sites had sampling problems due to additional landscape heterogeneity caused by small fire scars, roads, and clearings.

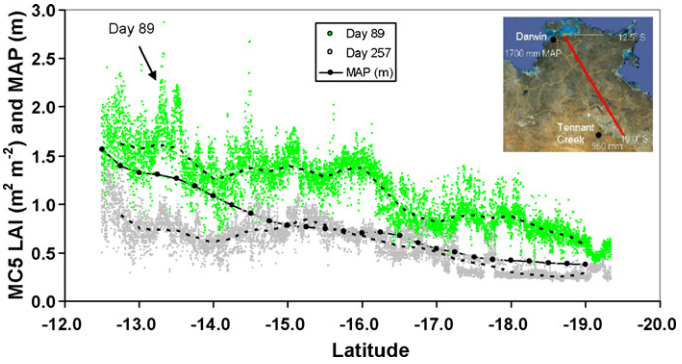

Fig. 6. Pattern of MC5 LAI along a transect in the Northern Territory, Australia (inset). Contrast is shown between MC5 LAI during the wet season (Day 89) and the dry season (Day 257). The MODIS pixel data were averaged over 0.25° latitudinal bands (dashed lines) along the transect from Howard Springs to just southeast of Tennant Creek. Mean Annual Precipitation (MAP) along the transect is depicted in m per year. Climate data (1961–90) courtesy of the Australian Bureau of Meteorology.

Table 3
Latitude, longitude, site description, and Leaf Area Index (LAI) from MC5 for bare ground or senescent grass sites in the Northern Territory. For the SPECIAL campaign, Site B corresponds to Daly River Pasture, Site C to Sturt Plains.

Site	Latitude	Longitude	Description	MODIS LAI
A	−14.0103	131.3646	Bare	0.3
B	−14.0631	131.3167	Senescent	0.5
C	−17.1517	133.3485	Senescent	0.2
D	−17.8974	133.9301	Bare	0.2
E	−17.9918	134.0157	Senescent	0.2
				Mean = 0.28 Std = 0.13

When these four sites were excluded the Root Mean Square Error (RMSE) for LAI was 0.16 $m^2\ m^{-2}$ indicating that MC5 LAI could be used effectively as input for modeling of carbon and water exchange across large regions. We acknowledge, however, that for sparsely vegetated sites, the relative errors may be large. Our results do show a small but significant LAI offset (0.146 $m^2\ m^{-2}$), when we included MODIS pixels known to contain bare ground or senescent grass (Table 2). We recognize that this effect is probably within the error limits of measurements and that it is insignificant when LAI > 3. However, a systematically high bias of LAI ~ 0.2 in sparser canopies could lead to predictions of a carbon sink where no active photosynthesis is taking place. Further measurements in sparse canopies are needed to confirm whether the bias observed in this study is more general.

Our results show a good relationship between MC5 LAI and estimates using digital hemispherical photographs that were analyzed by incorporating clumping. Although the correlation coefficients were virtually identical for SMA regressions using clumped and non-clumped LAI, errors using the clumping algorithm in CAN_EYE were largely unsystematic (random) compared to higher systematic errors (bias) with the non-clumping algorithm. Likewise, the slope of SMA regression between clumped LAI and MC5 LAI was approximately unity, while the slope for non-clumped LAI was significantly greater than one. This agrees well with Shabanov et al. (2005) and Ryu et al. (2010) who concluded that MC5 LAI measures green LAI and it captures aspects of clumping. This implies that ignoring clumping when analyzing DHP leads to a substantial underestimation of LAI.

Our results comparing MC5 LAI with hemispherical photos are promising and suggest that the current version of MODIS captures the phenology of savannas well both qualitatively and quantitatively. According to the MODIS Land Team Validation website (http://landval.gsfc.nasa.gov/) the validation status for LAI/fPAR (MOD15) is currently Stage 2: *product accuracy has been assessed over a widely distributed set of locations and time periods via several ground-truth and validation efforts*. Stage 3 validation could adopt the methodology of this study for rapid and independent estimates of LAI.

Our finding that approximately 21% of PAI is due to woody material (Fig. 4) agrees with studies by Dufrene and Breda (1995) and Scholes et al. (2004). The ability to quantify the woody component of PAI as a simple percentage of tree cover is promising for estimating the actual LAI needed for modeling carbon and water exchange. The relationship held across a wide range of tree cover levels in our study (~1–45%) and along the pronounced north–south rainfall gradient found in the Northern Territory. However, this is in contrast to previous literature suggesting that the woody component of measured LAI should increase along an aridity gradient (Scholes et al., 2004). Given the large number of papers addressing LAI, it is surprising that so few explicitly address effects of light interception by stems on estimates of LAI. More research is needed to see if, as suggested by our results, there is a general relationship between measure PAI and actual LAI.

We recognize that there are a number of sampling problems potentially influencing our results that need further discussion. (1) Ideally, one would be able separate leaf and non-leaf components to estimate a true leaf area index (Morisette et al., 2006; Fuentes et al., 2009). Though this is feasible for agricultural crops, with little structural material and downward focused photographs, tree canopy architecture generally leads to some obscuring of leaves by stems and branches. (2) Additionally photographs should be taken under uniformly clear skies or cloudy conditions to minimize sampling inconsistencies due to irregular illumination, including shadows (Macfarlane et al., 2007a). However, because time was limited during the field campaign, we sampled throughout the day, even though photographs often captured the sun directly. This was not a large problem because the CAN_EYE software allowed the masking of such distortions. (3) Although our measurements represent a snapshot in time for leaf area index, our study focuses on the direct comparison between two major methods for measuring leaf area: satellite and ground-based measurements. Despite these potential sampling problems, there is good agreement between DHP and MC5 estimates.

5. Conclusions

We have shown that MODIS LAI Collection 5.0 (MC5) provides a substantial improvement over the previous collection 4.8 for tropical savanna regions, as typified by results for a field site near Howard Springs, Northern Territory. Improvement was shown for both the timing and values of LAI when compared to ground-based estimates of LAI. There was good agreement between LAI from MC5 and LAI derived using the clumping algorithm in CAN_EYE software used to analyze digital hemispherical photographs. A significant positive offset of 0.146 $m^2\ m^{-2}$ exists in MC5 LAI when we included sites having bare ground or senescent grass. This study provides additional validation work that is rarely published in the literature, especially for low canopy vegetation in savannas or shrublands. The good agreement between MC5 LAI and ground-based estimates using hemispherical photos is highly encouraging and provides a basis for its use in assessing the spatial variability of leaf area index across the savanna landscapes of Australia.

Acknowledgements

This research was supported by a CSIRO Office of the Chief Executive postdoctoral research fellowship. We wish to also thank Drs. David Jupp and Tim McVicar for their comments on an earlier draft of the manuscript, and Mr. Steve Zegelin for help in the field.

References

Andrew, M.H., Noble, I.R., Lange, R.T., 1979. A non-destructive method for estimating the weight of forage on shrubs. Australian Rangelands Journal 1, 225–231.
Arora, V.K., Boer, G.J., 2005. A parameterization of leaf phenology for the terrestrial ecosystem component of climate models. Global Change Biology 11 (1), 39–59.

Asner, G.P., Scurlock, J.M.O., Hicke, J.A., 2003. Global synthesis of leaf area index observations: implications for ecological and remote sensing studies. Global Ecology and Biogeography 12 (3), 191–205.
Bacour, C., Baret, F., Beal, D., Weiss, M., Pavageau, K., 2006. Neural network estimation of LAI, fAPAR, fCover and LAIxC_{ab}, from the top of canopy MERIS reflectance data: principles and validation. Remote Sensing of Environment 105 (4), 313–325.
Baret, F., Weiss, M., 2004. Can-Eye: processing digital photographs for canopy structure characterization. CAN_EYE tutorial document, Avignon, France.
Baret, F., Hagolle, O., Geiger, B., Bicheron, P., Miras, B., Huc, M., Berthelot, B., Nino, F., Weiss, M., Samain, O., Roujean, J.L., Leroy, M., 2007. LAI, fAPAR, and fCover, CYCLOPES global products derived from VEGETATION: Part I. Principles of the algorithm. Remote Sensing of Environment 110 (3), 275–286.
Breda, N.J.J., 2003. Ground-based measurements of leaf area index: a review of methods, instruments and current controversies. Journal of Experimental Botany 54 (392), 2403–2417.
Chapin, F.S, Matson, P.A., Mooney, H.A., 2002. Principles of Terrestrial Ecosystem Ecology. Springer, New York.
Chen, J.M., Black, T.A., 1992. Defining leaf-area index for non-flat leaves. Plant, Cell and Environment 15 (4), 421–429.
Cleugh, H.A., Leuning, R., Mu, Q.Z., Running, S.W., 2007. Regional evaporation estimates from flux tower and MODIS satellite data. Remote Sensing of Environment 196 (3), 285–304.
Cohen, W.B., Maiersperger, T.K., Yang, Z., Gower, S.T., Turner, D.P., Ritts, W.D., Berterretche, M., Running, S.W., 2003. Comparisons of land cover and LAI estimates derived from ETM+ and MODIS for four sites in North America: a quality assessment of 2000/2001 provisional MODIS products. Remote Sensing of Environment 88 (3), 233–255.
Cohen, W.B., Maiersperger, T.K., Turner, D.P., Ritts, W.D., Pflugmacher, D., Kennedy, R.E., Kirschbaum, A., Running, S.W., Costa, M., Gower, S.T., 2006. MODIS land cover and LAI collection 4 product quality across nine sites in the western hemisphere. IEEE Transactions on Geoscience and Remote Sensing 44 (7), 1843–1857.
Cook, G.D., Heerdegen, R.G., 2001. Spatial variation in the duration of the rainy season in monsoonal Australia. International Journal of Climatology 21 (14), 1723–1732.
Cook, G.D., Williams, R.J., Hutley, L.B., O'Grady, A.P., Liedloff, A.C., 2002. Variation in vegetative water use in the savannas of the North Australian Tropical Transect. Journal of Vegetation Science 13 (3), 413–418.
Cramer, W., Kicklighter, D.W., Bondeau, A., Moore III, B., Churkina, G., Nemry, B., Ruimy, A., Schloss, A.L., 1999. Comparing global models of terrestrial net primary productivity (NPP): overview and key results. Global Change Biology 5 (Suppl. 1), 1–15.
Demarez, V., Duthoit, S., Baret, F., Weiss, M., Dedieu, G., 2008. Estimation of leaf area and clumping indexes of crops with hemispherical photographs. Agricultural and Forest Meteorology 128 (4), 644–655.
Demarty, J., Chevallier, F., Friend, A.D., Viovy, N., Paio, S., Ciais, P., 2007. Assimilation of global MODIS leaf area index retrievals within a terrestrial biosphere model. Geophysical Research Letters 34 (15), L15402.
Dufrene, E., Breda, N., 1995. Estimation of deciduous forest leaf area index using direct and indirect methods. Oecologia 104 (2), 156–162.
Fang, H., Liang, S., 2005. A hybrid inversion method for mapping leaf area index from MODIS data: experiments and application to broadleaf and needleleaf canopies. Remote Sensing of Environment 94 (3), 405–424.
Fuentes, S., Palmer, A.R., Taylor, D., Zeppel, M., Whitley, R., Eamus, D., 2009. An automated procedure for estimating the leaf area index (LAI) of woodland ecosystems using digital imagery, MATLAB programming and its application to an examination of the relationship between remotely sensed and field measurements of LAI. Functional Plant Biology 35 (9–10), 1070–1079.
Ganguly, S., Samanta, A., Schull, M.A., Shabanov, N.V., Milesi, C., Nemani, R.R., Knyazikhin, Y., Myneni, R.B., 2008. Generating vegetation leaf area index Earth system data record from multiple sensors. Part 2. Implementation, analysis and validation. Remote Sensing of Environment 112 (12), 4318–4332.
Garrigues, S., Lacaze, R., Baret, F., Morisette, J.T., Weiss, M., Nickeson, J.E., Fernandes, R., Plummer, S., Shabanov, N.V., Myneni, R.B., Knyazikhin, Y., Yang, W., 2008. Validation and intercomparison of global leaf area index products derived from remote sensing data. Journal of Geophysical Research 113 (G2), G02028, doi:10.1029/2007JG000635.
Gower, S.T., Cucharik, C.J., Norman, J.M., 1999. Direct and indirect estimation of leaf area index, fAPAR, and net primary production of terrestrial ecosystems. Remote Sensing of Environment 70 (1), 29–51.
Hill, M.J., Senarath, U., Lee, A., Zeppel, M., Nightingale, J.M., Williams, R.D.J., McVicar, T.R., 2006. Assessment of the MODIS LAI product for Australian ecosystems. Remote Sensing of Environment 101 (4), 495–518.
Huang, D., Knyazikhin, Y., Wang, W., Deering, D.W., Stenberg, P., Shabanov, N., Tan, B., Myneni, R.B., 2008. Stochastic transport theory for investigating the three-dimensional canopy structure from space measurements. Remote Sensing of Environment 112 (1), 35–50.
Huemmrich, K.F., Privette, J.L., Mukelabai, M., Myneni, R.B., Knyazikhin, Y., 2005. Time-series validation of MODIS land biophysical products in a Kalahari woodland, Africa. International Journal of Remote Sensing 26 (19), 4381–4398.
Jonckheere, I., Fleck, S., Nackaerts, K., Muys, B., Coppin, P., Weiss, M., Baret, F., 2004. Review of methods for in situ leaf area index determination. Part I. Theories, sensors and hemispherical photography. Agricultural and Forest Meteorology 121 (1–2), 19–35.
Kang, S., Running, S.W., Limb, J.-H., Zhao, M., Park, C.-R., Loehman, R., 2003. A regional phenology model for detecting onset of greenness in temperate mixed forests, Korea: an application of MODIS leaf area index. Remote Sensing of Environment 86 (2), 232–242.
Kanniah, K.D., Beringer, J., Hutley, L.B., Tapper, N.J., Zhu, X., 2009. Evaluation of collections 4 and 5 of the MODIS Gross Primary Productivity product and algorithm improvement at a tropical savanna site in northern Australia. Remote Sensing of Environment 113 (9), 1808–1822.
Knyazikhin, Y., Glassy, J., Privette, J.L., Tian, Y., Lotsch, A., Zhang, Y., Wang, Y., Morisette, J.T., Votava, P., Myneni, R.B., Nemani, R.R., Running, S.W., 1999. MODIS Leaf Area Index (LAI) and Fraction of Photosynthetically Active Radiation Absorbed by Vegetation (FPAR) Product (MOD15) Algorithm Theoretical Basis Document. Available from: <http://eospso.gsfc.nasa.gov/atbd/modistables.html>.
Lang, A.R.G., Xiang, Y.Q., 1986. Estimation of leaf-area index from transmission of direct sunlight in discontinuous canopies. Agricultural and Forest Meteorology 37 (3), 229–243.
Leblanc, S.G., Chen, J.M., Fernandes, R., Deering, D.W., Conley, A., 2005. Methodology comparison for canopy structure parameters extraction from digital hemispherical photography in boreal forests. Agricultural and Forest Meteorology 129 (3–4), 187–207.
Leuning, R., Cleugh, H.A., Zegelin, S.J., Hughes, D., 2005. Carbon and water fluxes over a temperate Eucalyptus forest and a tropical wet/dry savanna in Australia: measurements and comparison with MODIS remote sensing estimates. Agricultural and Forest Meteorology 129 (3–4), 151–173.
Leuning, R., Zhang, Y.Q., Rajaud, A., Cleugh, H., Tu, K., 2008. A simple surface conductance model using MODIS leaf area index and the Penman-Monteith equation. Water Resources Research 45 (10), W10419.
LI-COR, 1992. LAI-2000 Plant Canopy Analyzer Instruction Manual. LI-COR, Inc., Lincoln, Nebraska, USA.
Lu, H., Raupach, M.R., McVicar, T.R., Barrett, D.J., 2003. Decomposition of vegetation cover into woody and herbaceous components using AVHRR NDVI time series. Remote Sensing of Environment 86 (1), 1–18.
Macfarlane, C., Grigg, A., Evangelista, C., 2007a. Estimating forest leaf area using cover and fullframe fisheye photography: thinking inside the circle. Agricultural and Forest Meteorology 146 (1–2), 1–12.
Macfarlane, C., Hoffman, M., Eamus, D., Kerp, N., Higginson, S., McMurtrie, R., Adams, M., 2007b. Estimation of leaf area index in eucalypt forest using digital photography. Agricultural and Forest Meteorology 143 (3–4), 176–188.
Morisette, J.T., Baret, F., Privette, J.L., Myneni, R.B., Nickeson, J.E., Garrigues, S., Shabanov, N.V., Weiss, M., Fernandes, R.A., Leblanc, S.G., Kalacska, M., Sanchez-Azofeifa, G.A., Chubey, M., Rivard, B., Stenberg, P., Rautiainen, M., Voipio, P., Manninen, T., Pilant, A.N., Lewis, T.E., Iiames, J.S., Colombo, R., Meroni, M., Busetto, L., Cohen, W.B., Turner, D.P., Warner, E.D., Petersen, G.W., Seufert, G., Cook, R., 2006. Validation of global moderate-resolution LAI products: a framework proposed within the CEOS land product validation subgroup. IEEE Transactions on Geoscience and Remote Sensing 44 (7), 1804–1817.
Myneni, R.B., Hoffman, S., Knyazikhin, Y., Privette, J.L., Glassy, J., Tian, Y., Wang, Y., Song, X., Zhang, Y., Smith, G.R., Lotsch, A., Friedl, M., Morisette, J.T., Votava, P., Nemani, R.R., Running, S.W., 2002. Global products of leaf area index and fraction absorbed PAR from year one of MODIS data. Remote Sensing of Environment 83 (1–2), 214–231.
O'Grady, A.P., 2000. Patterns of tree and stand water use in the eucalypt open-forests of northern Australia. PhD Thesis, Charles Darwin University, Darwin, 163 pp.
O'Grady, A.P., Chen, X., Eamus, D., Hutley, L.B., 2000. Composition, leaf area index and standing biomass of eucalyptus open forests near Darwin in the Northern Territory, Australia. Australian Journal of Botany 48 (5), 629–638.
Privette, J.L., Myneni, R.B., Knyazikhin, Y., Mukelabai, M., Roberts, G., Tian, Y., Wang, Y., Leblanc, S.G., 2002. Early spatial and temporal validation of MODIS LAI product in the Southern Africa Kalahari. Remote Sensing of Environment 83 (1–2), 232–243.
Ryu, Y., Sonnentag, O., Nilson, T., Vargas, R., Kobayashi, H., Wenk, R., Baldocchi, D.D., 2010. How to quantify tree leaf area index in an open savanna ecosystem: a multi-instrument and multi-model approach. Agricultural and Forest Meteorology 150 (1), 63–76.
Scholes, R.J., Frost, P.G.H., Tian, Y., 2004. Canopy structure in savannas along a moisture gradient on Kalahari sands. Global Change Biology 10 (3), 292–302.
Shabanov, N.V., Huang, D., Yang, W., Tan, B., Knjazikhin, Y., Myneni, R.B., Ahl, D.E., Gower, S.T., Huete, A.R., Aragao, L.E.O.C., Shimabukuro, Y.E., 2005. Analysis and optimization of the MODIS leaf area index algorithm retrievals over broadleaf forests. IEEE Transactions on Geoscience and Remote Sensing 43 (8), 1855–1865.
Shabanov, N.V., Huang, D., Knjazikhin, Y., Dickinson, R.E., Myneni, R.B., 2007. Stochastic radiative transfer model for mixture of discontinuous vegetation canopies. Journal of Quantitative Spectroscopy & Radiative Transfer 107 (2), 236–262.
Sitch, S., Huntingford, C., Gedney, N., Levy, P.E., Lomas, M., Piao, S.L., Betts, R., Ciais, P., Cox, P., Friedlingstein, P., Jones, C.D., Prentice, I.C., Woodward, F.I., 2008. Evaluation of the terrestrial carbon cycle, future plant geography, and climate-carbon cycle feedbacks using five Dynamic Global Vegetation Models (DGVMs). Global Change Biology 14 (9), 2015–2039.
Stockli, R., Rutishauser, T., Dragoni, D., O'Keefe, J., Thornton, P.E., Jolly, M., Lu, L., Denning, A.S., 2008. Remote sensing data assimilation for a prognostic phenology model. Journal of Geophysical Research 113 (G4), G04021.
Tan, B., Woodcock, C.E., Hu, J., Zhang, P., Ozdogan, M., Huang, D., Yang, W., Knyazikhin, Y., Myneni, R.B., 2006. The impact of gridding artifacts on the local spatial properties of MODIS data: implications for validation, compositing, and

band-to-band registration across resolutions. Remote Sensing of Environment 105 (2), 98–114.
Wang, Y., Woodcock, C.E., Buermann, W., Stenberg, P., Voipio, P., Smolander, H., Hame, T., Tian, Y.H., Hu, J.N., Knyazikhin, Y., Myneni, R.B., 2004. Evaluation of the MODIS LAI algorithm at a coniferous forest site in Finland. Remote Sensing of Environment 91 (1), 114–127.
Warren Wilson, J., 1963. Estimation of foliage denseness and foliage angle by inclined point quadrats. Australian Journal of Botany 11, 95–105.
Warton, D.I., Wright, I.J., Falster, D.S., Westoby, M., 2006. Bivariate line-fitting methods for allometry. Biological Reviews 81 (2), 259–291.
Weiss, M., Baret, F., Smith, G.J., Jonckheere, I., Coppin, P., 2004. Review of methods for in situ leaf area index (LAI) determination. Part II. Estimation of LAI, errors and sampling. Agricultural and Forest Meteorology 121 (1–2), 37–53.
Williams, R.J., Duff, G.A., Bowman, D.M.J.S., Cook, G.D., 1996. Variation in the composition and structure of tropical savannas as a function of rainfall and soil texture along a large-scale climatic gradient in the Northern Territory, Australia. Journal of Biogeography 23 (6), 747–756.
Williams, R.J., Myers, B.A., Muller, M.J., Duff, G.A., Eamus, D., 1997. Leaf phenology of woody species in a northern Australian tropical savanna. Ecology 78 (8), 2542–2558.
Woinarski, J., Mackey, B., Nix, H., Traill, B., 2007. The Nature of Northern Australia. Australian National University Press, Canberra, Australia.
Yang, W., Huang, D., Tan, B., Stroeve, J.C., Shabanov, N.V., Knyazikhin, Y., Nemani, R.R., Myneni, R.B., 2006a. Analysis of leaf area index and fraction of PAR absorbed by vegetation products from the terra MODIS sensor: 2000–2005. IEEE Transactions on Geoscience and Remote Sensing 44 (7), 1829–1842.
Yang, W., Tan, B., Huang, D., Rautiainen, M., Shabanov, N.V., Wang, Y., Privette, J.L., Huemmrich, K.F., Fensholt, R., Sandholt, I., Weiss, M., Ahl, D.E., Gower, S.T., Nemani, R.B., Knyazikhin, Y., Myneni, R.B., 2006b. MODIS leaf area index products: from validation to algorithm improvement. IEEE Transactions on Geoscience and Remote Sensing 44 (7), 1885–1898.
Zhang, X., Friedl, M.A., Schaaf, C.B., Strahler, A.H., Hodges, J.C.F., Gao, F., Reed, B.C., Huete, A., 2003. Monitoring vegetation phenology using MODIS. Remote Sensing of Environment 84 (3), 471–475.